Influence of Surface Parameters on Anode Losses in Arcjets

H. A. Hassan* and Neill S. Smith†
North Carolina State University, Raleigh, N. C.

An analysis is presented in which the influence of the various surface parameters on the dominant mode of energy transfer to the anode, namely, that due to the electron current, is considered. It is found that, for the range of parameters investigated, the important parameters are the work function, the thermal accommodation coefficient, and diffuse reflection coefficients of the electrons, with the latter being important only for incomplete thermal accommodation. For typical degrees of ionization and a given current density, the anode loss decreases with an increase in the thermal accommodation coefficient and increases with an increase in the diffuse reflection coefficients; this behavior is a result of the necessary adjustment in the anode drop to maintain a fixed current density.

Introduction

THE high rates of heat transfer in arcjets result in reduced thermal efficiency and severely limit the lifetime of the electrodes. Because of thermionic emission, cathode losses are usually small and the bulk of the loss takes place through the anode. The dominant energy transfer to the anode is generally believed to be that due to the electron current.[1,2] Because such an energy flux is influenced by the anode surface conditions, an attempt is made to assess the influence of the various surface parameters on the anode loss and, in turn, identify the important parameters that affect the thermal efficiency.

The analysis is restricted to situations where the sheath thickness is less than the mean free paths and the Larmor radii. Because of the continuity of the fluxes at the sheath edge, the influence of the surface parameters on the anode loss can be obtained from a consideration of their influence on heat losses calculated from a collisionless sheath model which takes into consideration surface effects. The calculations presented here are based on a model similar to that developed in Ref. 3 and takes into consideration emission, reflection, surface ionization, and incomplete accommodation. The parameters investigated include the diffuse and specular reflection coefficients of particles coming from the sheath edge and the anode, thermal accommodation coefficients, pressure and degree of ionization at the sheath edge, and temperatures of incoming particles for tungsten and thoriated tungsten electrodes and lithium and argon propellants. To obtain quantitative results, one needs to assume a given anode drop or a given current density. Both of these possibilities are considered in this investigation.

It should be noted that, at present, values of the thermal accommodation coefficients and reflection coefficients for the energy range of interest (<10 ev) do not exist.[4,5] These coefficients vary, however, between zero and one and calculations were carried for such a range. The results shown in the figures are representative of the computations, and because of the lack of experimental data, direct comparison of this theory with experiment has not been possible.

Analysis

The steady-state motion of the particles in a collisionless sheath is governed by Vlasov's equations and Poisson's equation. An infinite planar anode with uniform work function is assumed; thus, the distribution functions and electrical potential are functions of the coordinate normal to the electrode. This assumption implies that the analysis is valid in those situations in which conditions along the anode do not vary appreciably in a distance of the order of a sheath thickness.

For a computation of the anode loss and current density, one needs to specify the distribution functions for the incident, reflected, trapped, and emitted particles and appropriate boundary conditions. The distribution functions are assumed Maxwellian; thus for the incident particles one can write

$$F_{i,j} = a_j \left(\frac{m_j}{2\pi k T_{i,j}}\right)^{1/2} H(\epsilon_j - e_j\phi)\,[H(e_j\phi_0 - \epsilon_j) + H(-u_j)H(\epsilon_j - e_j\phi_0)]\exp\left[\frac{-(\epsilon_j - e_j\phi_\infty)}{kT_{i,j}}\right] \qquad j = 1, 2, 3 \quad (1)$$

$H(z)$ is a step function which equals one when z is positive and zero otherwise; T is the temperature; k is the Boltzmann constant; e_j is the charge of species j; ϕ is the potential; m is the particle mass; and ϵ_j is given by

$$\epsilon_j = \tfrac{1}{2}m_j u_j^2 + e_j\phi \quad (2)$$

where u_j is the particle velocity normal to the electrode. Subscript i denotes an incident particle, subscripts 0 and ∞ refer to the anode surface and sheath edge, respectively, while subscripts 1, 2, and 3 denote electrons, ions, and atoms, respectively. The second part of Eq. (1) represents the distribution functions for electrons, atoms, and those ions with enough energy to reach the anode, while the first part represents the distribution function for ions unable to reach the anode. Similar expressions are written for diffusely reflected, trapped, and emitted particles but with a_j being replaced by b_j, c_1, and d_j, respectively.

The complete distribution functions and boundary conditions have been developed in detail in Ref. 3 and will not be reproduced here. The boundary conditions make it possible to express b_j, c_1, and d_j in terms of a_j. In addition, if charge neutrality is assumed at the sheath edge, then a_1, a_2, and a_3 can be expressed in terms of the pressure p and the degree of ionization α there. The results of the various manipulations are given in the Appendix.

For the assumed distribution functions, the current densities and heat fluxes can be expressed as

$$j_1 = e\,(kT_0/2\pi m_1)^{1/2}\,[a_1(1 - \alpha_{\infty,1})\,\theta_{i,1}{}^{1/2}\exp(-\epsilon_1{}^*/\theta_{i,1}) - b_1\theta_{d,1}{}^{1/2}\exp(-a/\theta_{d,1}) - d_1\exp(-a)] \quad (3)$$

Presented as Paper 69-107 at the AIAA 7th Aerospace Sciences Meeting, New York, January 20-22, 1969; submitted February 7, 1969; revision received October 3, 1969. Supported, in part, by NASA Grant NGR-34-002-048 and NSF Grant NXFGY-4460.

* Professor of Mechanical and Aerospace Engineering. Associate Fellow AIAA.

† Research Assistant.

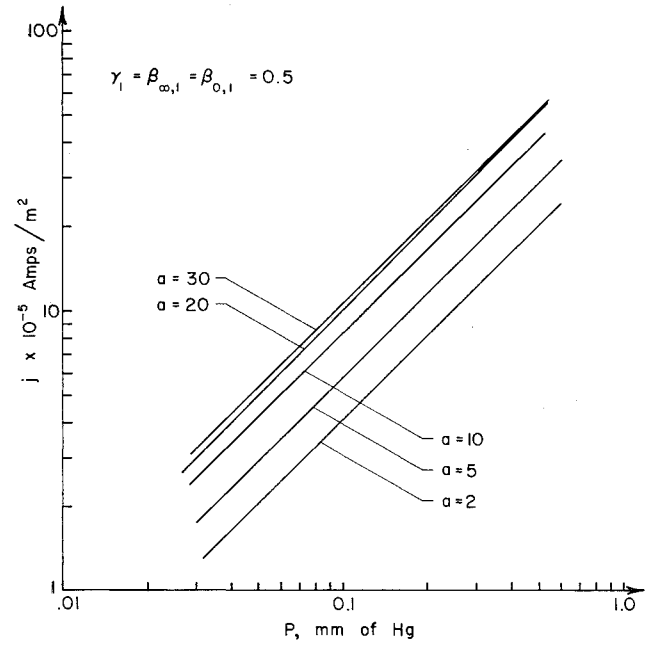

Fig. 1 Current density vs pressure.

$$j_2 = -e\,(kT_0/2\pi m_2)^{1/2}\,[a_2(1 - \alpha_{\infty,2} - \beta_{\infty,2})\theta_{i,2}^{1/2} \times \exp(-a/\theta_{i,2}) - d_2] \quad (4)$$

$$q_1 = kT_0\,(kT_0/2\pi m_1)^{1/2}\,[a_1(1 - \alpha_{\infty,1})\theta_{i,1}^{1/2}(\epsilon_1^* + 2\theta_{i,1} + a)\exp(-\epsilon_1^*/\theta_{i,1}) - b_1\theta_{d,1}^{1/2}(2\theta_{d,1} + a) \times \exp(-a/\theta_{d,1}) - d_1(2 + a)\exp(-a)] + j_1 w \quad (5)$$

$$q_2 = 2kT_0\,(kT_0/2\pi m_2)^{1/2}\,[a_2\,(1 - \alpha_{\infty,2})\theta_{i,2}^{3/2}\exp(-a/\theta_{i,2}) - b_2\theta_{d,2}^{3/2} - d_2] - j_2(I - w) \quad (6)$$

$$q_3 = 2kT_0\,(kT_0/2\pi m_3)^{1/2}\,[a_3(1 - \alpha_{\infty,3})\theta_{i,3}^{3/2} - b_3\theta_{d,3}^{3/2} - d_3] \quad (7)$$

Subscript d designates diffusely reflected particles, T_0 is the anode temperature, $\alpha_{\infty,s}$ and $\beta_{\infty,s}$ are the specular and diffuse reflection coefficients of particles coming from the sheath edge, w is the work function, I is the ionization potential, and

$$\theta = T/T_0,\ a = e(\phi_0 - \phi_\infty)/kT_0,\ \epsilon_1^* = m_1 u_1^{*2}/2kT_0 \quad (8)$$

where u_1^* is the minimum velocity of incoming electrons.

When a becomes large, the current density approaches a saturation current density which can be approximated, from Eqs. (3) and (4), by

$$j_{\text{sat.}} = e\left(\frac{kT_0}{2\pi m_1}\right)^{1/2} a_1(1 - \alpha_{\infty,1})\theta_{i,1}^{1/2}\exp\left(\frac{-\epsilon_1^*}{\theta_{i,1}}\right) \quad (9)$$

Similarly, Eqs. (5–7) show that, at saturation, the anode loss is proportional to the saturation current density. Examination of the expression for a_1, which is given by Eq. (A6), indicates that for the range of parameters investigated, it is proportional to p/kT_0 (Fig. 1). Thus, at saturation, both the current density and anode loss are proportional to p.

Results and Discussion

For all practical purposes, the contribution of ions and neutrals to the heat flux is negligible, and so is the contribution of the ion current to the total current. Therefore, of all the reflection and thermal accommodation coefficients appearing in the theory, only those associated with electrons are investigated. Also, because specular reflection coefficients are usually small for typical surfaces, all were set equal to 0.05 for the results presented below. Other parameters investigated include the temperature of incoming electrons, anode temperature, pressure and degree of ionization at the sheath edge for tungsten and thoriated tungsten anodes and argon and lithium propellants. The results indicate that, although the type of propellant has an appreciable influence on the ion and the neutral contribution to the heat flux, it has very little influence on the electron contribution and thus on the total heat flux. This would indicate that, for a given current, the thermal efficiency is practically independent of the propellant.[6] Therefore, all the results presented below are for argon.

Before discussing the influence of the various surface parameters on the anode loss, attention is directed to Fig. 1, which shows a plot of the current density vs pressure for various anode drops. Because of the current saturation, there is a limited range of allowable currents for a given pressure; thus random selection of current density and pressure at the sheath edge is not possible. It is also seen that for current densities of 10–100 amps/cm^2, the pressure in the neighborhood of the anode has to be very low. The calculations presented here are for a pressure of 0.1 mm Hg at the anode sheath.

Figures 2 and 3 show plots of q and j vs $\beta_{\infty,1}$ for the various values of the thermal accommodation coefficient γ_1 and $\beta_{0,1}$, at a given (dimensionless) anode drop, a. The voltage drop kT_0a, is not to be confused with the "effective" anode voltage drop defined as the ratio of the power loss to the arc power. To interpret these figures, it is noted that the number of diffusely reflected electrons increases with both $\beta_{0,1}$ and $\beta_{\infty,1}$, and any increases in the diffusely reflected electrons will result in a decrease in the heat flux and the current density. Because the energy given up by the electrons increases with γ_1, the reflected particles will have less energy to overcome the potential barrier, and this will result in an increase in j. Figure 2 shows that when γ_1 is close to unity, the anode loss is insensitive to the various reflection coefficients; conversely, when it is not close to unity, a large reduction in the anode loss can be realized.

Nerheim and Kelly[7] concluded, after examining available thermal efficiency data, that the assumption of a constant anode drop is questionable. Therefore a given current density instead of anode drop is assumed next. The conservation of charge equation in the bulk of the plasma, $\nabla \cdot \mathbf{j} = 0$, reduces for an infinite planar electrode to $dj/dx = 0$ or $j =$ const where x is the coordinate normal to the electrode. The justification for assuming a constant current density follows from the continuity of the current density at the sheath edge. It is expected that this assumption will remain

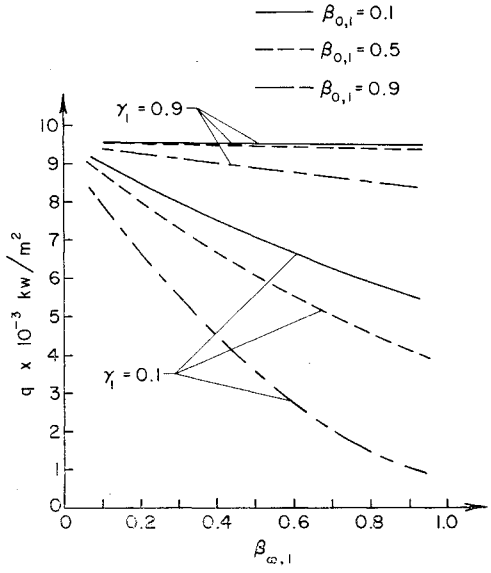

Fig. 2 Effect of surface parameters on anode loss ($a = 10$).

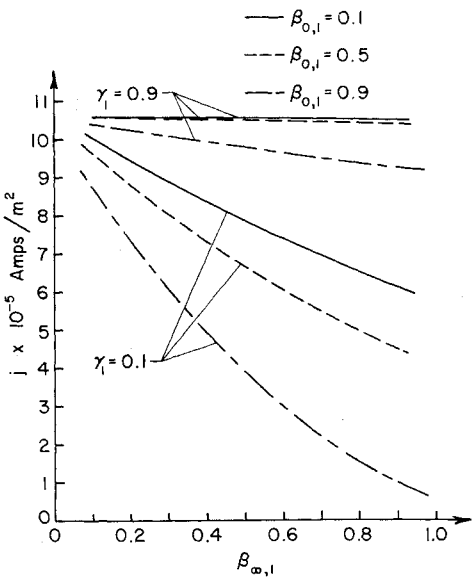

Fig. 3 Effect of surface parameters on current density (a = 10).

plausible as long as changes along the electrodes are small compared to those normal to the electrode. However, this may not be the case in all arcjets. The results shown in Figs. 4–9 are for a given current density. Figures 4 and 5 show a plot of the anode loss vs $\beta_{\infty,1}$ and γ_1 for various values of $\beta_{0,1}$ and J, where J designates the fraction of the saturation current density, which is about 100 amps/cm^2, at the assumed pressure. It is seen that q decreases with γ_1 and increases with $\beta_{\infty,1}$ and $\beta_{0,1}$. This behavior of q is opposite to that indicated in Fig. 2, where the anode drop and not the current density was assumed given. The reason for this behavior follows from the consideration that an increase in $\beta_{0,1}$ and $\beta_{\infty,1}$ results in an increase in the number of diffusely reflected particles. However, to maintain the same current

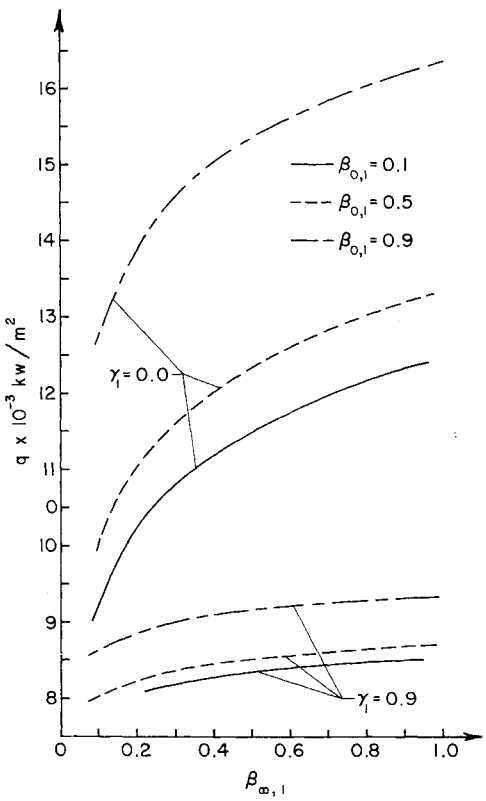

Fig. 4 Influence of reflection on anode loss.

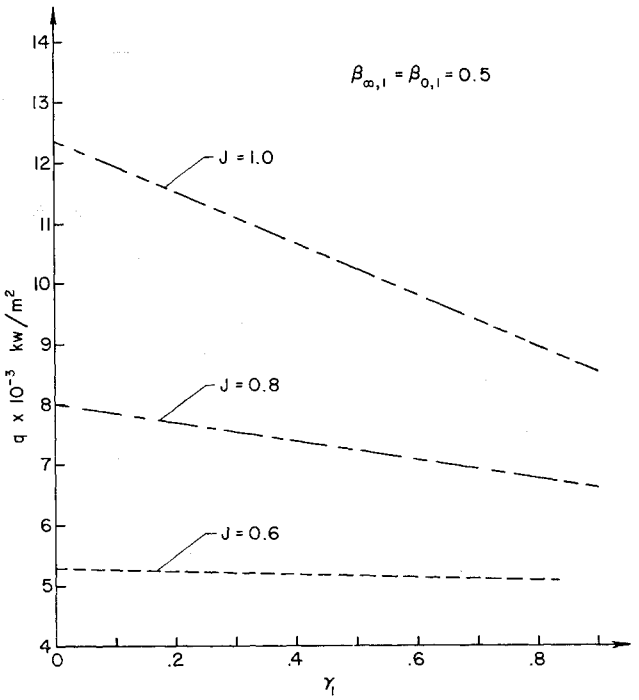

Fig. 5 Influence of thermal accommodation and current density on anode loss.

density more particles have to reach the wall; this can be achieved, as is seen from Fig. 6, by a larger anode drop. The resulting increase in the kinetic energy of the current carrying electrons is responsible for the observed behavior of q with $\beta_{0,1}$ and $\beta_{\infty,1}$. On the other hand, an increase in γ_1 results in a decrease in the number of electrons leaving the anode sheath and thus a smaller number of particles have to reach the wall to maintain a constant current density. Figure 5 also shows that the quantity q/j, which is equal to the effective anode drop, is not constant.

The influence of the anode temperature on the anode loss is shown in Fig. 7. An increase in the anode surface temperature results in more emission, and thus a decrease in the net current to the wall. To maintain a constant current

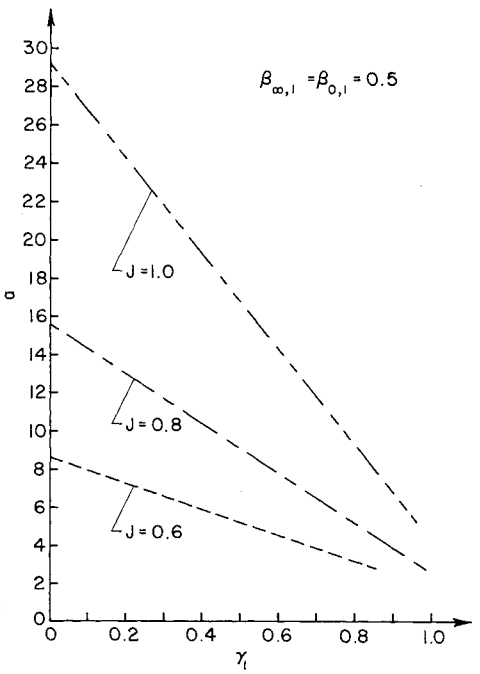

Fig. 6 Anode drop vs thermal accommodation coefficient.

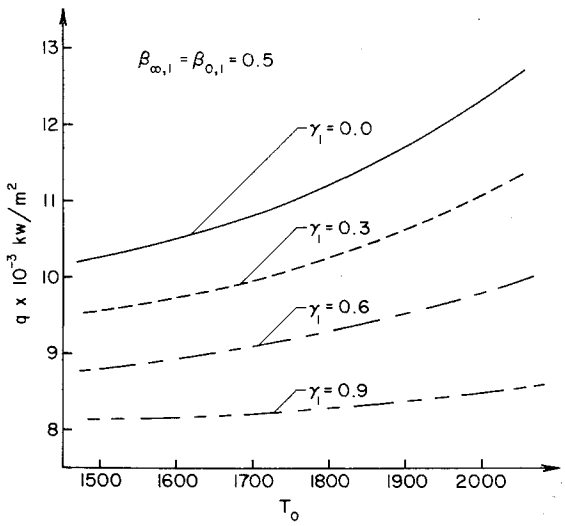

Fig. 7 Anode loss vs anode temperature.

density, the anode drop has to increase, resulting in more energetic electrons reaching the anode surface; this results in an increase in the anode loss. Figure 8 shows, as expected, that q increases with the electrode work function and the temperature of the incident electrons.

The preceding results were obtained for a degree of ionization at the sheath edge, α, of 0.05. The influence of this parameter is shown in Fig. 9 for various values of γ_1. An increase in α, at given pressure and temperatures, results in an increase in number of electrons. To maintain the current density at the assumed level, the anode drop will decrease and this will result in a decrease in q. The figure also shows that, for the higher degrees of ionization, q increases with γ_1; as α increases, the sheath drop becomes so small that its influence on the anode loss is negligible. Thus, the particles behave in a manner similar to that in the absence of a potential drop. Because of the low anode drops associated with the high degrees of ionization (less than 1 ev), it is concluded that, for typical operations at the assumed pressure where the anode drop was estimated to be in the range 4–8 volts,[8] the degree of ionization at the anode sheath is probably less than 5%.

Concluding Remarks

If the electrons behave like light noble atoms, which are characterized by low thermal accommodation coefficients,[5] then surface effects can have a large influence on the anode loss. In this case, the dominant parameters are the work function and the diffuse reflection coefficients for the electrons. On the other hand, if the electron thermal accommodation coefficient is close to unity, then the surface parameters have little influence on the thermal efficiency. Definite conclusions will have to wait detailed measurements of electron reflection and thermal accommodation coefficients and their effect on anode losses.

Appendix

Using the boundary conditions given in Ref. 3, the coefficients b_j, c_1, and d_j appearing in the assumed distribution functions can be written as

$$b_1 = \frac{1}{\chi\theta_{d,1}^{1/2}}\left\{a_1(1-\alpha_{0,1})\beta_{\infty,1}\theta_{i,1}^{1/2}\exp\left(\frac{-\epsilon_1^*}{\theta_{i,1}}\right) + d_1\beta_{0,1}[1-\exp(-a)]\right\}$$

$$c_1 = \{a_1\beta_{\infty,1}\theta_{i,1}^{1/2}\exp(-\epsilon_1^*/\theta_{i,1})[1-\exp(-a/\theta_{d,1})] + d_1[1-\exp(-a)]\}\{\theta_{t,1}\chi[1-\exp(-a/\theta_{t,1})]\}^{-1}$$

$$d_1 = \left\{4\left(\frac{2\pi m_1 kT_0}{h^2}\right)^{3/2}\exp\left(\frac{-w}{kT_0}\right)\right\}\{1+\operatorname{erf}a^{1/2}\}^{-1} \quad \text{(A1)}$$

$$b_2 = a_2\beta_{\infty,2}(\theta_{i,2}/\theta_{d,2})^{1/2}\exp(-a/\theta_{i,2})$$

$$d_2 = \nu d_3 \quad \text{(A2)}$$

$$b_3 = a_3\beta_{\infty,3}(\theta_{i,3}/\theta_{d,3})^{1/2}$$

$$d_3 = (1/1+\nu)[a_2(1-\alpha_{\infty,2}-\beta_{\infty,2})\theta_{i,2}^{1/2}\exp(-a/\theta_{i,2}) + a_3(1-\alpha_{\infty,3}-\beta_{\infty,3})\theta_{i,3}^{1/2}] \quad \text{(A3)}$$

where

$$\chi = 1-\alpha_{0,1}-\beta_{0,1}[1-\exp(-a/\theta_{d,1})]$$

$$\nu = (g_2/g_3)\exp[-(I-w)/kT_0] \quad \text{(A4)}$$

and $\alpha_{0,s}$ and $\beta_{0,s}$ are the specular and diffuse reflection coefficients of particles coming from the anode, h is Planck's constant, and g is the degeneracy of the ground state.

Assuming charge neutrality at the sheath edge, a_1, a_2, and a_3 can be expressed in terms of the pressure, p, and the degree of ionization, α, at the sheath edge. Thus, setting

$$n_1 = n_2,\ p = \sum_j\sum_r kn_{r,j}T_{r,j},\ n_2/n_3 = \alpha/(1-\alpha) \text{ at } \phi = \phi_\infty \quad \text{(A5)}$$

one finds

$$a_j = \lambda_{j1}(a_1X_{11}+A_1),\ j = 2,3$$

$$a_1 = [(p/kT_0) - B_1 - \lambda_{21}Y_{22} - \lambda_{31}Y_{33}] \times [Y_{11} + (\lambda_{21}Y_{22}+\lambda_{31}Y_{33})X_{11}]^{-1} \quad \text{(A6)}$$

where

$$X_{11} = (1/2\chi\theta_{d,1}^{1/2})\beta_{\infty,1}(1-\alpha_{0,1})\theta_{i,1}^{1/2}\exp(-a/\theta_{d,1}) \times \exp(-\epsilon_1^*/\theta_{i,1}) + \tfrac{1}{2}(1+\alpha_{\infty,1})\operatorname{erfc}(\epsilon_1^*/\theta_{i,1})^{1/2}$$

$$\lambda_{21} = \left[X_{33} - \frac{1-\alpha}{\alpha}\right]X_{32}[X_{22}X_{33} - X_{23}X_{32}]^{-1}$$

$$\lambda_{31} = \left[\frac{1-\alpha}{\alpha}X_{22} - X_{23}\right][X_{22}X_{33} - X_{23}X_{32}]^{-1}$$

$$X_{22} = \operatorname{erf}\left(\frac{a}{\theta_{i,2}}\right)^{1/2} + \tfrac{1}{2}(1+\alpha_{\infty,2})\operatorname{erfc}\left(\frac{a}{\theta_{i,2}}\right)^{1/2} + \frac{\beta_{\infty,2}}{2}\left(\frac{\theta_{i,2}}{\theta_{d,2}}\right)^{1/2}\operatorname{erfc}\left(\frac{a}{\theta_{d,2}}\right)^{1/2}\exp\left[-\frac{a}{\theta_{i,2}}+\frac{a}{\theta_{d,2}}\right] + \frac{\nu}{2(1+\nu)}(1-\alpha_{\infty,2}-\beta_{\infty,2})\theta_{i,2}^{1/2}\exp(a)\operatorname{erfc}a^{1/2} \times \exp\left(\frac{-a}{\theta_{i,2}}\right)$$

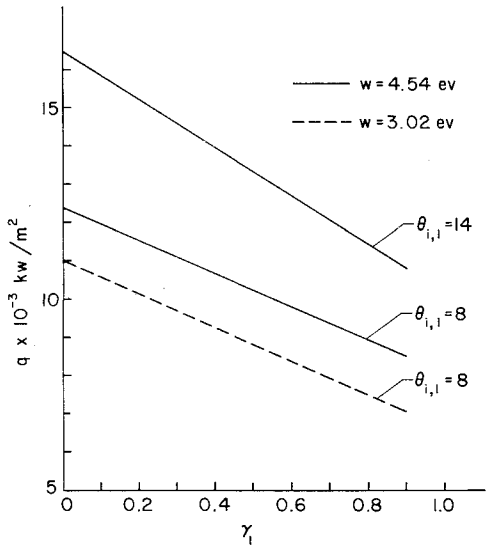

Fig. 8 Effect of work function and temperature of incident electrons on anode loss.

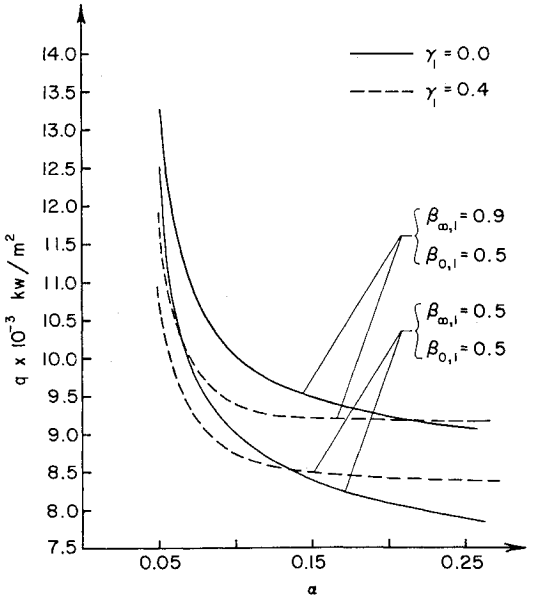

Fig. 9 Influence of degree of ionization on anode loss.

$$X_{23} = [\theta_{i,2}^{1/2}/2(1+\nu)](1-\alpha_{\infty,2}-\beta_{\infty,2})\exp(-a/\theta_{i,2})$$

$$X_{32} = \frac{\nu}{2(1+\nu)}(1-\alpha_{\infty,3}-\beta_{\infty,3})\theta_{i,3}^{1/2}\exp(a)\,\mathrm{erfc}a^{1/2}$$

$$X_{33} = \tfrac{1}{2}\beta_{\infty,3}(\theta_{i,3}/\theta_{d,3})^{1/2}[\theta_{i,3}^{1/2}/2(1+\nu)] \times (1-\alpha_{\infty,3}-\beta_{\infty,3}) + \tfrac{1}{2}(1+\alpha_{\infty,2})$$

$$A_1 = d_1\{\tfrac{1}{2}\exp(-a) + (\beta_{0,1}/2\chi\theta_{d,1}^{1/2}) \times [1-\exp(-a)]\exp(-a/\theta_{d,1})\}$$

$$B_1 = d_1\{\tfrac{1}{2}\exp(-a) + (\beta_{0,1}\theta_{d,1}^{1/2}/2\chi) \times [1-\exp(-a)]\exp(-a/\theta_{d,1})\}$$

$$Y_{11} = (\theta_{d,1}^{1/2}/2\chi)(1-\alpha_{0,1})\beta_{\infty,1}\theta_{i,1}^{1/2} \times \exp(-a/\theta_{d,1})\exp(-\epsilon_1^*/\theta_{i,1}) + (1+\alpha_{\infty,1})\theta_{i,1}\,\mathrm{erfc}(\epsilon_1^*/\theta_{i,1})^{1/2}$$

$$Y_{22} = \theta_{i,2}\,\mathrm{erf}(a/\theta_{i,2})^{1/2} + \tfrac{1}{2}(1+\alpha_{\infty,2})\theta_{i,2} \times \mathrm{erfc}\left(\frac{a}{\theta_{i,2}}\right)^{1/2} + \frac{\beta_{\infty,2}}{2}\theta_{d,2}\left(\frac{\theta_{i,2}}{\theta_{d,2}}\right)^{1/2}$$

$$Y_{33} = \tfrac{1}{2}(1+\alpha_{\infty,3})\theta_{i,3} + \tfrac{1}{2}\beta_{\infty,3}\left(\frac{\theta_{i,3}}{\theta_{d,3}}\right)^{1/2}\theta_{d,3} + \frac{1}{2(1+\nu)}(1-\beta_{\infty,3}-\alpha_{\infty,3})\theta_{i,3}^{1/2}[1+\nu\exp(a)\,\mathrm{erfc}a^{1/2}]$$

References

[1] Cann, G. L. et al., "Hall Current Accelerator," Rept. 5470-Final, NASA CR-54705, 1966 Electro-Optical Systems, Pasadena, Calif.

[2] Shih, K. T. et al., "Experimental Anode Heat-Transfer Studies in a Coaxial Arc Configuration," *AIAA Journal*, Vol. 6, No. 8, Aug. 1968, pp. 1482–1487.

[3] Hassan, H. A., "Surface Effects on the Structure of a Collisionless Sheath Near an Electrode," *The Physics of Fluids*, Vol. 11, No. 5, May 1968, pp. 1085–1091.

[4] McDaniel, E. W., *Collision Phenomena in Ionized Gases*, 1st ed., Wiley, New York, 1964, Chap. 13.

[5] Kaminsky, M., *Atomic and Ionic Impact Phenomena on Metal Surfaces*, 1st ed., Academic Press, New York, 1965, Chaps. 6 and 11.

[6] John, R. R. and Bennett, S., "Arc Jet Technology Research and Development," AVCO/RAD SR-65-37, NASA CR-54687, 1965, AVCO Corp., Research and Advanced Development Div. (now AVSSD), Wilmington, Mass.

[7] Nerheim, N. M. and Kelly, A. J., "A Critical Review of the State-of-the-Art of the MPD Thrustor," AIAA Paper 67-688, Colorado Springs, Colo., 1967.

[8] Shih, K. T., "Anode Current and Heat Flux Distributions in an MPD Engine," AIAA Paper 69-244, Williamsburg, Va., 1969.